HHS Public Access

Author manuscript

Curr Eye Res. Author manuscript; available in PMC 2017 July 01.

Published in final edited form as:

Curr Eye Res. 2016 July ; 41(7): 977–986. doi:10.3109/02713683.2015.1083588.

Defining the relationships among retinal function, layer thickness and in visual behavior during oxidative stress-induced retinal degeneration

Amit K. Patel, **Elizabeth Akinsoji**, and **Abigail S. Hackam**

Abstract

Purpose—The purpose of this study was to identify how changes in retinal structure and function correlate with visual deficits during increasing amounts of retinal degeneration.

Materials and Methods—Retinal degeneration was induced in adult mice by subretinal injections of paraquat (0.2–1 mM). Retinal anatomy and photoreceptor layer thickness were quantified by histology and optical coherence tomography, retinal function was measured using electroretinography, and visual behavior were measured by optokinetic tracking, at 1–3 weeks post-injury.

Results—Photoreceptor layer structure, function, and visual behavior declined at a linear rate over time following paraquat induced degeneration, with the correlations between outcome measures being lowest at mild injury levels and increasing with injury severity. Overall reductions in visual acuity were highly correlated with declines in retinal thickness (r^2=0.78) and function (r^2=0.67) and retinal thickness correlated with photoreceptor function (r^2=0.72). ERG a-wave scotopic amplitudes showed a stronger correspondence to in retinal structure and visual behavior than b-waves.

Conclusions—Measurements of photoreceptor loss at the structural and functional levels showed good correspondence with degeneration-associated changes in visual behavior after oxidative stress injury. The results provide new insight about the relative kinetics of measurements of retinal degeneration induced by oxidative stress, which could guide the choice of optimal outcome measurements for other retinal diseases.

Keywords

Retinal degeneration; optical coherence tomography (OCT); electroretinography (ERG); optokinetic tracking (OKT); oxidative stress

INTRODUCTION

Many retinal diseases, including age-related macular degeneration and retinitis pigmentosa, are caused by progressive retinal cell loss. In most cases, irreversible deficits in vision have

Corresponding author: Abigail S. Hackam, Bascom Palmer Eye Institute, University of Miami Miller School of Medicine, McKnight Bldg. Rm. 407, 1638 NW 10th Ave., Miami, FL 33136, Tel: (305) 547-3723, Fax: (305) 547-3658, ahackam@med.miami.edu.

DECLARATION OF INTEREST

The authors declare they have no competing interests.

already occurred by the time loss of retinal structure has been detected.[1, 2, 3, 4] Therefore, an important focus in the field is defining the kinetics of structural and functional degenerative changes, and characterizing the amount of degeneration that leads to visual deficits.[3] Determining the extent that functional, structural and histological outcome measures of retinal degeneration relate to declines in vision behavior would indicate which outcome measures are most appropriate to use at different stages of degeneration, and could guide experimental analysis of therapeutic interventions.

There is a general lack of understanding of how changes to retina structure and function correspond to the degree of visual deficits. Although several studies have characterized the rates of degeneration at structural and functional levels for various retinal injuries[2, 4, 5, 6], very few reports have precisely correlated these different outcome measurements. For example, analysis of the *rd10* mouse model of retinal degeneration described declining structural and functional loss of photoreceptors[7], but the extent that these two measurement outcomes compared with each other was not determined. A correlational analysis of patients with retinal degeneration demonstrated that structural and functional measurements, obtained using fdOCT and mfERG respectively, showed increasing correlation as the disease progresses; however, it remains unknown exactly how the two measures correlate with remaining visual activity.[1]

Changes in visual behavior in animal models are often assessed using optokinetic tracking (OKT), which measures an animal's reflex behavior to track, and therefore see, moving objects.[8, 9, 10] The OKT assay is a well-characterized technique that is used to detect the level of visual acuity in many vertebrates organisms, including mice and humans.[8, 11, 12, 13, 14] However, the extent that visual behavior decline correlates with changes in retinal structure and function is still not clear.

A major cause of retinal degeneration is elevated oxidative stress, which occurs in photoreceptor diseases and in numerous retinal and neuronal degeneration models.[15, 16, 17, 18] While the effects of oxidative stress in the retina have been widely studied[15, 19, 20, 21], the temporal relationship between oxidative stress and initiation of visual deficits remain unknown. A commonly used chemical compound to model oxidative stress in the retina is paraquat (PQ), or 1,1'-Dimethyl-4,4'-bipyridinium dichloride. PQ generates oxygen radicals through redox cycling and NADPH oxidase regulation[22] and intravitreal injections of PQ lead to degeneration and decreased function of photoreceptors and ganglion cells.[19, 23] PQ offers the advantage over genetic models in that different degrees of injury can be induced with different doses at the same age of the animal, thus avoiding age-dependent effects.[24]

In this study, we examined the degree of correlation among measurements of retinal photoreceptor degeneration and visual degradation, using an oxidative stress induced retinal degeneration mouse model. We found a dose-dependent linear decline of vision, and a high positive correlation among photoreceptor structure and function and visual acuity measurements, indicating that quantifying changes in structure or function correspond well with changes in visual acuity. Furthermore, the coefficient of determination dose-dependently increased with the concentration of oxidative stress, indicating that the different

measurement techniques are more correlative with increasing injury. Therefore, this study defines the relationship between structural, functional and visual decline during oxidative injury induced photoreceptor degeneration.

MATERIALS AND METHODS

Animals

All animal work adhered to the regulations of the ARVO Statement for the Use of Animals in Ophthalmic and Vision Research and was approved by the Animal Care and Use Committee at the University of Miami. Wild type mice (strain B6;129SF2/J, The Jackson Laboratory, Bar Harbor, ME) of both sexes were used. Mice at age 3 months were anaesthetized using ketamine/xylazine and eyes were locally anesthetized with 0.5% proparacaine hydrochloride eye drops (Akorn, Lake Forest, IL). For subretinal injections, a small incision was made in the conjunctiva and sclera and a 1.5 cm 33-gauge Hamilton needle (Hamilton Company, Reno, NV) was inserted into the subretinal space in the superior region of the eye, using a microscope for visualization. Two microliters of PBS, or PQ (Sigma, St. Louis, MO) at increasing doses ranging from 0.2–1 mM were injected.[23, 25] Each mouse was injected in the same area of the eye. The average amount of cellular loss was similar among eyes measured at the same dose of PQ and time point, although the specific pattern of PQ-induced damage was not uniform between each eye. Subretinal injections generated transient retinal detachments that subsided by the 1 week time point, which was confirmed by OCT on each injected animal. Mice with unresolved retinal detachments or bleeding were excluded from further analysis. Investigators were masked to the identity of the injected compound for all analyses.

Histological analysis

Eyes were enucleated immediately after the mice were euthanized and fixed in 0.4% fresh paraformaldehyde then processed through a sucrose gradient (5%–20% sucrose in PBS).[26] The entire globe was sectioned into 10 μm cross-sections, stained with 4',6-diamidino-2-phenylindole (DAPI) to visualize the retina cell nuclei, and columns of photoreceptor nuclei in the ONL were counted near the optic nerve head and in the periphery in 5 sections, each approximately 200 μm apart.[23, 25] Central photoreceptors were counted approximately 200–300 μm from the optic nerve and peripheral photoreceptors were counted 200–300 μm from the end of the retina/ciliary epithelium.

For bipolar cell counts, immunostaining was performed as in Yi et al. using a rabbit antibody against protein kinase C (1:200 Santa Cruz Biotechnology, Inc., Dallas, TX) and goat-anti-rabbit Alexa 546 (1:600 Santa Cruz Biotechnology, Inc.) antibody.[26] Sections were counterstained using DAPI for nuclei labeling and imaged using a Zeiss Axiovert 200 fluorescent microscope at 20× magnification.

Retina layer thickness measurement using optical coherence tomography (OCT)

Mouse retinas were imaged non-invasively using a spectral domain optical coherence tomography (SD-OCT) system (Bioptigen, Research Triangle Park, NC) that was optimized for small animals. The mice were anaesthetized, wrapped in a blanket, and placed on the

OCT imaging stage.[27] The eyes were dilated with 10% topical phenylephrine eye drops and kept moist using artificial tears (Systane, Alcon, TX). Imaging scans covered a volume of $1.3 \times 1.3 \times 1.56\ mm^3$ of the mouse eye centered on the optic disk and 100 b-scans were generated, and b-scan density was 1000 a-scans/b-scan. Photoreceptor layer thickness was quantified using MATLAB (Mathworks, Natick, MA) and segmentation software and applications developed by the Ophthalmic Biophysics Center at the Bascom Palmer Eye Institute, University of Miami.[27] The thickness of the outer nuclear layer and inner and outer segments of the photoreceptors were measured in 70–80 cross-sectional b-scans and then averaged across the retina.[23, 28]

Retina function measurement using electroretinography (ERG)

The mice were dark adapted for 4 hours and were then anesthetized, wrapped in a heating blanket with a continuously running water bath to maintain a consistent body temperature and placed on the ERG stage. The eyes were dilated and kept moist, as described above. A grounding electrode was inserted into the tail of the mouse while the reference electrode was inserted under the skin between the eyes. Silver wire electrodes were placed on the corneas of the mice. Mice were exposed to flashes of white light ranging from 0.01 to 10 $cd•s/m^2$ in the scotopic range using a Ganzfeld light emitting chamber.[23, 29] For simplicity of the comparisons and correlations described below, all analyses were performed using the ERG recordings from the 1 $cd•s/m^2$ intensity, which was the intensity at which the photoreceptor responses reached maximal amplitudes. Field potentials generated by the retina were recorded from both eyes simultaneously using ten 250 μs flashes per light intensity with an interstimulus time of 5 seconds between each flash, and the responses to the ten flashes were averaged. Individual recordings at each of the flashes within the 10 recording showed no signs of diminishment with this interstimulus interval (Supplemental Figure 1). Flash intensity, duration and response recordings were conducted using the UTAS system controlled by EM for Windows software (LKC Technologies, Gaithersburg, MD). Notch filtering was used to reduce the 60 Hz signal noise. Low cut filtering was performed at 0.3 Hz and high cut filtering was performed at 500 Hz. Retinal function was assessed by measuring the average peak amplitude from the ERG waveforms. Oscillatory potential measurements were generated using the UTAS program under the same conditions as the ERG recordings, and filtering for oscillatory potentials (OP) was performed using the built in software filtering system based upon International Society for Clinical Electrophysiology of Vision (ISCEV) Standards[30]. The OP filtering did not significantly alter the ERG b-wave amplitudes at the light intensity used (Supplemental Table 6).

Visual behavior assessment

Optokinetic tracking measurements were performed by placing the mice on a raised platform in the center of a box surrounded by four monitors displaying rotating sinusoidal gratings of alternating white and black columns, following the method of Prusky et al.[31] and described previously.[23] The direction of column rotation was changed a total of 6 times with 30 seconds between each change. To determine the threshold response, column thickness was decreased step-wise by a factor of 1.5 until the animal could no longer track the column rotation. Mouse vision behavior was scored based on whether or not the animal could track the direction of column rotation with their head. The movement of the mice was monitored

by two observers who were masked to the identity of the treatment of each animal. Mouse visual acuity was defined as the highest spatial frequency that generated a consistent response from the mouse.

Statistical analysis

Determination of statistical significance among PQ concentrations at each time point was performed using ANOVA with Tukey's post-hoc test (Figures 1B, 3A, 3C, and 5A) using GraphPad Prism software (GraphPad Software, Inc, La Jolla, CA). Linear correlation and regression were used to address the relationships between specific bivariate parameters and dose, including rate of degeneration (Figure 1C, 3B, 3D, and 5B) and comparisons between different outcome measures (Figures 3E, 4, and 6) and was calculated using Microsoft Excel. Statistical significance between slopes was determined using the analysis of covariance (ANCOVA) test. Data points (retinal thickness, ERG amplitudes, and visual acuity) used in the regression analyses were generated from the same animal at a particular time and dose. P values <0.05 were considered significant.

RESULTS

Time- and dose-dependent changes in retinal thickness and function during retinal degeneration

In this study, we quantified and compared the rates of retinal degeneration using specific outcome measures at the structural, functional and behavioral levels to determine how reductions in retinal thickness and function correlate with vision deficits over the course of disease. To cause specific amounts of injury in adult animals of the same age, we induced retinal degeneration using the oxidative stress reagent PQ. Retinal changes were measured using optical coherence tomography (OCT), photoreceptor counts and electroretinography (ERG), which are well-established methods in the field, and have a large dynamic range that allows quantification of low and high levels of degeneration.

Visualization of the retina by OCT showed significant changes in the photoreceptor layer of eyes injected with PQ over time. As expected, thinning of the photoreceptor layer was mild at low doses and early time points, and degeneration progressively increased with time and dose. At the lowest concentration of PQ (0.2 mM) there was a 0.01 mm (10%) reduction in thickness of the photoreceptor layer at the 3 week time point. At the highest concentration (1 mM), photoreceptor layer thickness was reduced by 0.06 mm (57%), which was significantly different than the 0.2 mM concentration (Figure 1B, $p<0.05$, $n=5$). Control treatments, in which eyes were injected with PBS, maintained a constant average thickness over time. The average photoreceptor thickness among animals at each dose and time point showed low variation (Figure 1C, Supplemental Table 1).

In addition to the amount of degeneration, the average rate of degeneration across the time course of the study also increased with PQ dose (Table 1, slopes), ranging from 0.004 mm/week at 0.2 mM PQ to 0.02 mm/week at 1 mM PQ, resulting in a reduction of retinal thickness by 0.02mm/week per millimolar of PQ. The average changes in thickness across the entire retina were statistically significant with respect to PQ dosage and time (Figure 1B,

Supplemental Table 1). Regression analysis showed a linear decline of photoreceptor layer thickness over time at each concentration (Table 1) and a linear increase in the rate of degeneration with respect to increasing concentration (Figure 1C, r^2=0.98).

We next used an independent method of quantifying retinal degeneration by counting the number of remaining photoreceptors. While the histology of eyes injected with PBS did not change during the duration of the study, eyes injected with PQ showed a dose-dependent reduction in cell number in the outer nuclear layer (Figure 2). At the lowest concentration (0.2 mM), retinas had an average photoreceptor density of 3.13×10^5 cells/mm^2 in the outer nuclear layer compared with an average of 3.87×10^5 cells/mm^2 in retinas of eyes injected with PBS (19% loss, $p<0.05$, n=3). Eyes injected with 1 mM PQ had an average of 1.9×10^5 cells/mm^2, indicating a severe amount of photoreceptor cell death (52% cell loss compared with PBS injected eyes, $p<0.05$, n=3), which is similar to the amount of loss observed by OCT. A comparison of slopes by ANCOVA showed a difference in rate of degeneration between central and peripheral photoreceptor loss with respect to concentration. Therefore, the photoreceptor counts and OCT provided equivalent measurements of retinal degeneration despite using different parameters. Furthermore, rod bipolar cell counts showed a similar trend as the photoreceptors, with 1.2×10^4 cells/mm^2 in PBS injected eyes, which decreased to 5.1×10^3 cells/mm^2 in the 1mM PQ injected eyes (58 % cell loss, $p<0.05$, n=3) (Fig 2C,D), indicating that PQ also had a dose-dependent effect on the inner retina.

The functional decline of the retina in response to induction of retinal oxidative stress was quantified using flash ERG. For simplicity of the correlation analyses below, we compared ERG recordings from the intensity of 1 cd•s/m^2, which was the intensity at which the photoreceptor responses reached maximal amplitude. Retinal function, as measured by a-waves (photoreceptors) and b-waves (bipolar cells and inner retina), showed a dose-dependent decrease with increasing PQ concentration (Figure 3A,C,F), similar to the reductions in retinal thickness and photoreceptor counts. The ERG waveforms generated in the PBS-injected mice maintained similar shapes and amplitudes over the duration of the study (Figure 3A, C). The ERG a-wave amplitude decreased by 8% at the lowest concentration of PQ (0.2 mM) compared with PBS at the three week time point, which was similar to the reductions in the retina thickness (Figure 1) and photoreceptor counts (Figure 2). In contrast, at the highest concentration of PQ, there was a much greater reduction in a-wave amplitude (92% functional loss compared with PBS, $p<0.05$, n=5, Figure 3A, Supplemental Table 2) compared with the structural degeneration (57% reduction of photoreceptor layer thickness and 52% loss in photoreceptor counts), indicating that functional loss shows a higher rate of decline, measured by ERG, compared with structural loss, measured by OCT. Furthermore, the ERG b-wave response had a much greater decrease than the a-waves at the lowest concentration of PQ (40% loss of amplitude at 0.2 mM vs. 8% loss for a-waves, compared with PBS, $p<0.05$, n=5, Figure 3C, Supplemental Table 3). At the highest concentration of PQ, the reduction of the b-wave amplitude was similar to the reduction of the a-wave with an 86% loss (1.0 mM PQ compared with PBS, $p<0.05$, n=5). Analysis of oscillatory potentials showed no significant difference between the PQ concentrations (Supplemental Table 6). Therefore, dose-dependent reductions in

retinal function due to PQ injury, measured by ERG, show a greater dynamic range than structural loss, measured by OCT.

In addition to the amount of degeneration, the rate of degeneration also increased with PQ dose (Table 1, slopes), when measured at the functional level, and ranged from an average loss of 16 μV/week at 0.2 mM PQ to 50 μV/week for the a-waves at 1mM PQ over the entire three week period. A regression analysis indicated that retinal function declined with a linear trend at each concentration (Table 1). The average rate of functional decline in both the a-wave and b-wave amplitudes over time also followed a linear trend with respect to increasing concentration (r^2=0.95 for a-wave and r^2=0.76 for b-wave, Figure 3B, D). We also examined the correlation between a-wave and b-wave amplitudes among individual concentrations (all concentrations and time points), and determined that the functional loss correlated well between the a-wave and b-wave at low concentrations (r^2=0.77, Figure 3E), but did not correlate well at higher concentrations of PQ (r^2=0.29) (Table 2). While the slopes of the b-wave amplitudes with respect to concentration did have a strong linear correlation (r^2=0.76), the graph in Figure 3D indicates a possible non-linear component as well, which may contribute to the correlation between the a- and b-wave weakening at higher concentrations.

Comparing all concentrations and time points together demonstrated a high correlation between OCT and ERG amplitudes (r^2=0.72 for OCT and a-wave, r^2=0.68 for OCT and b-wave) (Figure 4A, B). Although there is a significant difference ($p<0.05$) between the absolute percentage of structural and functional loss at the highest concentration (57% loss in thickness and 92% loss in a-wave amplitude), the rate at which these measurements decline is comparable. The decline in both measurements followed a linear pattern with high overall correlation. There was significant correlation between OCT and both ERG waves starting at 0.4 mM of PQ ($p<0.05$), as measured by regression analysis. Analysis of individual concentrations in the a-wave amplitudes showed moderately high correlation across the majority of the concentrations (0.4 mM and higher, $p<0.05$). Together, these results show that PQ induced photoreceptor functional decline occurs at a similar rate as photoreceptor structural decline.

Examination of the coefficient of determination between OCT and ERG a-waves at each concentration showed a dose-dependent increase with concentration (Table 2), which indicates that changes to retinal thickness and function are more comparable at higher concentrations of PQ. In contrast, correlation coefficients and coefficients of determination between OCT and ERG b-waves at each concentration did not increase in a dose-dependent manner (Table 2). Instead, the coefficient of determination at each concentration remained fairly constant, indicating that the power of the comparison between the ERG b-wave for retinal structure does not increase with concentration (Table 2). A reason for this observation is that the a-wave is a direct measure of photoreceptor activity and therefore is likely to correlate better with photoreceptor layer thickness. In contrast, the b-wave is modulated by a number of influences in addition to bipolar cell integrity and photoreceptor input, including Muller glia and inhibitory neurons.[32, 33] Therefore, changes to any of these factors may alter the b-wave amplitude, resulting in lower correlations with photoreceptor layer thickness.

Quantification of changes in visual behavior during increasing amounts of retinal degeneration

Visual behavior was measured using the optokinetics tracking (OKT) response. Because vision is the ultimate result of signaling of all the retinal cells, we expected visual behavior to show greater deterioration with increasing oxidative insult. Indeed, at the 3 week time point, there is a 13% loss of visual behavior at the lowest concentration (0.2 mM) and a 94% loss of visual behavior at the highest concentration (1 mM) (Figure 5, Supplemental Table 4). The loss of visual acuity closely matches the decline in photoreceptor function as measured by the ERG a-wave (8% loss at 0.2 mM and 92% loss at 1mM). Although the total amount of visual acuity loss at the lowest and highest concentration of PQ closely matched the loss of the ERG a-wave amplitude, the rate of decline of acuity did not follow a linear pattern (defined as a constant slope between time points) as the rate of functional decline did. We found that the decline of visual acuity measured by the OKT response could be fit to both a linear or logarithmic model at higher concentrations (0.6 mM and above) resulting in equivalent correlation coefficients. Fitting the correlation analysis of the slopes to a linear regression model for all concentrations demonstrated that mouse visual acuity across the different concentrations showed a linear correlation (r^2=0.92). Therefore, similar to the structural and functional changes, optokinetic visual behavior declined in a dose-dependent manner over time, as expected.

Visual acuity correlates with changes in retinal structure and function

A comparison of the correlations between measurements of photoreceptor degeneration and visual behavior by OCT and OKT, respectively, showed a high overall linear correlation (r^2=0.78) (Figure 6). A regression analysis between OCT and OKT at individual concentrations revealed a significant correlation starting at 0.4 mM PQ ($p<0.05$). However, examination of the correlation between OCT and OKT at individual concentrations over time revealed a poor Pearson's coefficient of determination at low concentrations of oxidative insult (r^2=0.22 at 0.2 mM), whereas the correlation is increased during higher levels of injury (r^2=0.51 at 1 mM). These results indicate that at higher levels of degeneration, the changes in photoreceptor structure are a better indicator of changes to visual acuity. A reason for the low correlation between OCT and OKT at low levels of degeneration could be due to the ceiling effect of the OKT. We found that maximum biological limit of visual acuity of the mice in this study peaked at 0.5 c/deg. Therefore, early changes in structure may not have been disruptive enough to influence overall visual loss and therefore retained high visual acuity, which would influence the level of correlation between OCT and OKT.

A comparison of how well retinal function correlates with visual behavior revealed moderately high correlations between the ERG amplitudes and visual acuity when examining all concentrations and time points together (r^2=0.67 for visual acuity and a-wave, r^2=0.60 for visual acuity and b-wave) (Figure 6). A regression analysis between ERG and OKT at individual concentrations revealed significant correlations at 0.6 mM PQ and higher for the a-waves, and 0.4 mM and higher for the b-waves ($p<0.05$). Based on the pattern of correlations between OCT and ERG and the pattern between OCT and OKT, it is likely that the functional response of the retina would similarly correlate with visual behavior. Indeed,

correlations between ERG a-wave and OKT at individual concentrations revealed lower correlations at low concentrations of oxidative injury (r^2=0.26 for visual acuity and a-wave), which increased as the concentration increased (r^2=0.61 for visual acuity and a-wave), which was similar to the comparison between OKT and OCT. In contrast, correlational analysis between the ERG b-wave and OKT showed a fairly constant, low correlation across concentrations (r^2=0.25 at 0.2 mM, r^2=0.24 at 1 mM PQ). These results indicate that the visual acuity changes correspond better to the a-wave than the b-wave, as expected because the b-wave is influenced by several different cell types.

DISCUSSION

The purpose of this study was to compare time- and dose-dependent effects of oxidative stress-induced retinal degeneration on retinal structure, function and visual behavior, and to identify the level of degeneration at which retinal changes result in visual deficits. The high correlation among photoreceptor degeneration measured by OCT, photoreceptor function measured by ERG a-waves, and visual behavior measured using OKT, demonstrated that declines in structure and function correspond to decreased visual behavior but that there were differences in dynamic range among measurement methods, and that the correlative value among these techniques is stronger with higher amounts of injury.

Regarding retinal function, we found that while the ERG scotopic a-waves correlate well with retinal structure and visual behavior, the ERG scotopic b-wave does not show high correlation with photoreceptor layer thickness or visual acuity. The reason is most likely because the a-wave is directly related to photoreceptor function and thus photoreceptor layer thickness, whereas the b-wave is influenced by several different cell types, including rod bipolar cells in the INL, which decreased with increasing PQ concentration. Therefore, the b-wave may show higher deficits at lower concentrations due to the loss of both photoreceptors and bipolar cells, as well as impairment of other inner retina cells such as Muller glia and inhibitory neurons. At higher concentrations of PQ, much of the photoreceptor functionality is greatly diminished, resulting in no signal for the remaining bipolar cells to respond to leading to similar levels of measured functional loss. Future studies would examine the relationships of the b-wave to changes in OCT and histological measurements of the inner retina and their correlation with visual acuity. Furthermore, although the a-waves showed strong correlation with retinal structure and visual behavior, if the remaining photoreceptors are less sensitive to light due to the oxidative stress injury, then their ability to signal to bipolar cells would also be reduced. It would be interesting in future studies to determine whether altered light sensitivity could be an early indicator of future decline in visual acuity in this animal model.

We also observed that the dynamic range of PQ-induced degeneration varied with measurement technique. While structural loss resulted in a decrease of 57% at the 3 week time point, photoreceptor function decreased by 92%. Interestingly, loss of function has been reported to occur prior to structural loss[34, 35, 36, 37], which may be an explanation for the difference in why retinal function and visual acuity decrease more than photoreceptor layer thickness at the 1 week time point.

To our knowledge, this is the first study to examine in depth the relationship between retinal structure, function, and visual behavior at increasing amounts of injury. The analysis of the OCT, ERG and OKT measurements indicated that the correlation between visual behavior and other measurements of retinal degeneration increased with injury. As the concentration of paraquat increased, the correlation between visual behavior and retinal structure or function increased in a linear manner, indicating that at low concentrations the measurements of structure, function, and vision do not correlate well but at increased levels of damage the correlation between measurements is high. Also, the degree of degeneration identified by the different outcome measures (OCT, ERG and OKT) is similar at low concentrations but different at the higher concentrations, as indicated by absolute loss of thickness, amplitude, or spatial frequency. However, as the level of oxidative stress increased, the correlational value between the techniques increased, indicating the variation among the measures of retinal degeneration in individual mice by different techniques decreased with amount of injury.

The results from our study are supported by previous findings in patients with various retinal abnormalities that were compared using multifocal electroretinogram (mfERG) and frequency domain optical coherence tomography (fdOCT), in which a low correlation between the techniques was observed in patients with early disease or small retinal abnormalities.[1] The patients in the study by Dale et al. were categorized into groups by the level of degeneration in the retina measured at the structural level by fdOCT and were assigned an independent categorical group based on severity of functional degeneration measured by mfERG. The correlation between the group assignments assessed by fdOCT and mfERG revealed that there was moderate correlation between categorizing degeneration using these two techniques across different levels of injury; however, the correlation was poor at low levels of degeneration, similar to our findings.

Our study, using a simple injury model, showed that visual behavior decreased in a linear manner over a course of three weeks in all the different concentrations. When the rate of degeneration is plotted according to the concentration, we see that the rate of decline in visual behavior is also linear (Figure 1B, 3B, 3D, and 5B). The linearity of the rate of visual behavior degeneration and concentration indicate that the level of visual behavior loss corresponds to measurements of retinal structure or function in a concentration-dependent manner. Identifying whether the model of the rate of degeneration fits a linear or exponential model is important for understanding and predicting the progression of disease and vision loss.[8] Previous studies in humans showed both linear and exponential declines in ocular function, using visual field, visual acuity and retinal function measurements[3839] and rates of choroidal neovascular lesion expansion in age-related macular degeneration patients.[4041] The complex nature of retinal diseases such as retinitis pigmentosa and AMD may contribute to the differing rates of degeneration.

The inherent differences in the retinas of mice and humans, such as distribution and ratios of the photoreceptor cells, may account for some of the differences in the rates of degeneration between these models and measurements. Human subjects allow for more complex visual behavior measurements, such as visual field tests and multifocal ERG, which provides more detailed mapping of degeneration in the retina. In this study, we examined visual behavior

using the optokinetic reflex, which is a gross measurement of visual acuity that is often used in studies on small mammals and invertebrates such as zebrafish and Drosophila. While the OKT assay is useful for assessing vision among animals of the same species, it is not yet understood how mouse acuity measured by the OKT compares with human acuity because mice lack a macula.[31, 42]

The death of photoreceptors due to PQ exposure is likely direct and other cell types possibly influencing the rate or amount of degeneration. Because other cell types are likely influenced by PQ, this study demonstrated the overall effect of PQ on the retina with respect to structure, function and visual behavior, rather than measuring photoreceptor death exclusively. Although some of these measurement endpoints are specific to photoreceptors (a-waves, ONL nuclei counts), other measurement endpoints clearly are not (visual acuity, b-waves). Therefore, we were able to quantify how photoreceptor layer structure and photoreceptor function correlate to the overall state of retinal function and vision. Indeed, the loss of cells in the INL supports the idea that the combined damage to multiple cells within the retina can lead to high correlations among different endpoints. Further studies are necessary to identify how other cell types, such as RPE and RGCs, influence the rate of photoreceptor degeneration and the effect on visual acuity in this model. The RPE regulate photoreceptor survival and function during normal conditions[43] and could play a role in oxidative stress-induced photoreceptor degeneration.[20] Although it is likely that RPE is affected by PQ-induced oxidative stress, it is unclear to what extent injury to these cells influences photoreceptor viability. PQ affects a wide range of cells in the retina, but it has been shown that the RPE is able to survive exposure to PQ extremely well compared with other cell types.[44] It is also possible that reduced RGC function from PQ may also influence the overall decline in visual acuity and future studies could be performed to quantify the dose- and time-dependent changes to RGC numbers and function and their correlations with visual acuity. In conclusion, this study provides a comprehensive measurement of how different amounts of retinal degeneration contribute to declines in visual behavior. These findings may help guide future studies to examine whether other acute injury models or progressive genetic models exhibit similar patterns and correlations as the PQ model, and whether the structural and functional techniques employed here can be used to predict changes in visual behavior in degenerations of other retinal cell types, such as RGCs.

Supplementary Material

Refer to Web version on PubMed Central for supplementary material.

Acknowledgments

FUNDING

This study was supported by a Research to Prevent Blindness Ernest & Elizabeth Althouse Special Scholar Award, the Karl Kirchgessner Foundation, NIH grant RO1 EY017837, and a Fight for Sight Student Fellowship. Institutional support to BPEI was from a Research to Prevent Blindness Unrestricted Grant and an NEI Center Core Grant P30 EY014801. The optokinetic device was designed and built at BPEI's Ophthalmic Biophysics Center by Victor E Hernandez MSBME and Jean-Marie Parel PhD with support from the Florida Lions Eye Bank, Karl R. Olsen, MD and Martha E. Hildebrandt, PhD and the Henri and Flore Lesieur Foundation (JMP).

Assistance with OCT analysis techniques was provided by Dr. Marco Ruggeri and the Ophthalmic Biophysics Center of University of Miami. We are grateful to William J. Feuer and Joyce Schiffman, Biostatistics Core Facility, Bascom Palmer Eye Institute, for guidance with statistical analysis.

REFERENCES

1. Dale EA, Hood DC, Greenstein VC, Odel JG. A comparison of multifocal ERG and frequency domain OCT changes in patients with abnormalities of the retina. Doc Ophthalmol. 2010; 120:175–186. [PubMed: 20043188]
2. Real JP, Granero GE, De Santis MO, Juarez CP, Palma SD, Kelly SP, et al. Rate of vision loss in neovascular age-related macular degeneration explored. Graefes Arch Clin Exp Ophthalmol. 2014
3. Keane PA, de Salvo G, Sim DA, Goverdhan S, Agrawal R, Tufail A. Strategies for improving early detection and diagnosis of neovascular age-related macular degeneration. Clin Ophthalmol. 2015; 9:353–366. [PubMed: 25733802]
4. Nagy D, Schonfisch B, Zrenner E, Jagle H. Long-term follow-up of retinitis pigmentosa patients with multifocal electroretinography. Invest Ophthalmol Vis Sci. 2008; 49:4664–4671. [PubMed: 18566474]
5. Clarke G, Collins RA, Leavitt BR, Andrews DF, Hayden MR, Lumsden CJ, et al. A one-hit model of cell death in inherited neuronal degenerations. Nature. 2000; 406:195–199. [PubMed: 10910361]
6. de Sisternes L, Simon N, Tibshirani R, Leng T, Rubin DL. Quantitative SD-OCT imaging biomarkers as indicators of age-related macular degeneration progression. Invest Ophthalmol Vis Sci. 2014; 55:7093–7103. [PubMed: 25301882]
7. Rosch S, Johnen S, Muller F, Pfarrer C, Walter P. Correlations between ERG, OCT, and Anatomical Findings in the rd10 Mouse. J Ophthalmol. 2014; 2014:874751. [PubMed: 24683495]
8. McGill TJ, Prusky GT, Douglas RM, Yasumura D, Matthes MT, Lowe RJ, et al. Discordant anatomical, electrophysiological, and visual behavioral profiles of retinal degeneration in rat models of retinal degenerative disease. Invest Ophthalmol Vis Sci. 2012; 53:6232–6244. [PubMed: 22899760]
9. Pearson RA, Barber AC, Rizzi M, Hippert C, Xue T, West EL, et al. Restoration of vision after transplantation of photoreceptors. Nature. 2012; 485:99–103. [PubMed: 22522934]
10. Prusky GT, Douglas RM. Developmental plasticity of mouse visual acuity. Eur J Neurosci. 2003; 17:167–173. [PubMed: 12534981]
11. McGill TJ, Prusky GT, Luna G, LaVail MM, Fisher SK, Lewis GP. Optomotor and immunohistochemical changes in the juvenile S334ter rat. Exp Eye Res. 2012; 104:65–73. [PubMed: 23036564]
12. Aung MH, Kim MK, Olson DE, Thule PM, Pardue MT. Early visual deficits in streptozotocin-induced diabetic long evans rats. Invest Ophthalmol Vis Sci. 2013; 54:1370–1377. [PubMed: 23372054]
13. Tabata H, Shimizu N, Wada Y, Miura K, Kawano K. Initiation of the optokinetic response (OKR) in mice. J Vis. 2010; 10
14. Thomas BB, Seiler MJ, Sadda SR, Coffey PJ, Aramant RB. Optokinetic test to evaluate visual acuity of each eye independently. J Neurosci Methods. 2004; 138:7–13. [PubMed: 15325106]
15. Moreira PI, Smith MA, Zhu X, Nunomura A, Castellani RJ, Perry G. Oxidative stress and neurodegeneration. Ann N Y Acad Sci. 2005; 1043:545–552. [PubMed: 16037277]
16. Shen JK, Dong A, Hackett SF, Bell WR, Green WR, Campochiaro PA. Oxidative damage in age-related macular degeneration. Histol Histopathol. 2007; 22:1301–1308. [PubMed: 17701910]
17. Izzotti A, Bagnis A, Sacca SC. The role of oxidative stress in glaucoma. Mutat Res. 2006; 612:105–114. [PubMed: 16413223]
18. Shen J, Yang X, Dong A, Petters RM, Peng YW, Wong F, et al. Oxidative damage is a potential cause of cone cell death in retinitis pigmentosa. J Cell Physiol. 2005; 203:457–464. [PubMed: 15744744]
19. Cingolani C, Rogers B, Lu L, Kachi S, Shen J, Campochiaro PA. Retinal degeneration from oxidative damage. Free Radic Biol Med. 2006; 40:660–669. [PubMed: 16458197]

20. Cai J, Nelson KC, Wu M, Sternberg P Jr, Jones DP. Oxidative damage and protection of the RPE. Prog Retin Eye Res. 2000; 19:205–221. [PubMed: 10674708]
21. Hollyfield JG, Bonilha VL, Rayborn ME, Yang X, Shadrach KG, Lu L, et al. Oxidative damage-induced inflammation initiates age-related macular degeneration. Nat Med. 2008; 14:194–198. [PubMed: 18223656]
22. Bus JS, Gibson JE. Paraquat: model for oxidant-initiated toxicity. Environ Health Perspect. 1984; 55:37–46. [PubMed: 6329674]
23. Patel AK, Hackam AS. A novel protective role for the innate immunity Toll-Like Receptor 3 (TLR3) in the retina via Stat3. Mol Cell Neurosci. 2014; 63C:38–48. [PubMed: 25264029]
24. Gao H, Hollyfield JG. Aging of the human retina. Differential loss of neurons and retinal pigment epithelial cells. Invest Ophthalmol Vis Sci. 1992; 33:1–17. [PubMed: 1730530]
25. Patel AK, Surapaneni K, Yi H, Nakamura RE, Karli SZ, Syeda S, et al. Activation of Wnt/beta-catenin signaling in Muller glia protects photoreceptors in a mouse model of inherited retinal degeneration. Neuropharmacology. 2014; 91C:1–12. [PubMed: 25486619]
26. Yi H, Patel AK, Sodhi CP, Hackam DJ, Hackam AS. Novel role for the innate immune receptor Toll-like receptor 4 (TLR4) in the regulation of the Wnt signaling pathway and photoreceptor apoptosis. PLoS One. 2012; 7:e36560. [PubMed: 22615780]
27. Ruggeri M, Wehbe H, Jiao S, Gregori G, Jockovich ME, Hackam A, et al. In vivo three-dimensional high-resolution imaging of rodent retina with spectral-domain optical coherence tomography. Invest Ophthalmol Vis Sci. 2007; 48:1808–1814. [PubMed: 17389515]
28. Camp AS, Ruggeri M, Munguba GC, Tapia ML, John SW, Bhattacharya SK, et al. Structural correlation between the nerve fiber layer and retinal ganglion cell loss in mice with targeted disruption of the Brn3b gene. Invest Ophthalmol Vis Sci. 2011; 52:5226–5232. [PubMed: 21622702]
29. Li Y, Tao W, Luo L, Huang D, Kauper K, Stabila P, et al. CNTF induces regeneration of cone outer segments in a rat model of retinal degeneration. PLoS One. 2010; 5:e9495. [PubMed: 20209167]
30. McCulloch DL, Marmor MF, Brigell MG, Hamilton R, Holder GE, Tzekov R, et al. ISCEV Standard for full-field clinical electroretinography (2015 update). Doc Ophthalmol. 2015; 130:1–12. [PubMed: 25502644]
31. Prusky GT, Alam NM, Beekman S, Douglas RM. Rapid quantification of adult and developing mouse spatial vision using a virtual optomotor system. Invest Ophthalmol Vis Sci. 2004; 45:4611–4616. [PubMed: 15557474]
32. Li J, Patil RV, Verkman AS. Mildly abnormal retinal function in transgenic mice without Muller cell aquaporin-4 water channels. Invest Ophthalmol Vis Sci. 2002; 43:573–579. [PubMed: 11818406]
33. Stockton RA, Slaughter MM. B-wave of the electroretinogram. A reflection of ON bipolar cell activity. J Gen Physiol. 1989; 93:101–122. [PubMed: 2915211]
34. Porciatti V, Ventura LM. Retinal ganglion cell functional plasticity and optic neuropathy: a comprehensive model. J Neuroophthalmol. 2012; 32:354–358. [PubMed: 23196946]
35. Caicedo A, Espinosa-Heidmann DG, Hamasaki D, Pina Y, Cousins SW. Photoreceptor synapses degenerate early in experimental choroidal neovascularization. J Comp Neurol. 2005; 483:263–277. [PubMed: 15682400]
36. Hilton KJ, Cunningham C, Reynolds RA, Perry VH. Early Hippocampal Synaptic Loss Precedes Neuronal Loss and Associates with Early Behavioural Deficits in Three Distinct Strains of Prion Disease. PLoS One. 2013; 8:e68062. [PubMed: 23840812]
37. Laliberte AM, MacPherson TC, Micks T, Yan A, Hill KA. Vision deficits precede structural losses in a mouse model of mitochondrial dysfunction and progressive retinal degeneration. Exp Eye Res. 2011; 93:833–841. [PubMed: 21983042]
38. Massof R, Finkelstein D. A two stage hypothesis for the natural course of retinitis pigmentosa. Advances in the Biosciences. 1987; 62
39. Berson EL, Rosner B, Weigel-DiFranco C, Dryja TP, Sandberg MA. Disease progression in patients with dominant retinitis pigmentosa and rhodopsin mutations. Invest Ophthalmol Vis Sci. 2002; 43:3027–3036. [PubMed: 12202526]

40. Liu TY, Shah AR, Del Priore LV. Progression of lesion size in untreated eyes with exudative age-related macular degeneration: a meta-analysis using Lineweaver-Burk plots. JAMA Ophthalmol. 2013; 131:335–340. [PubMed: 23494038]
41. Yehoshua Z, Rosenfeld PJ, Gregori G, Feuer WJ, Falcao M, Lujan BJ, et al. Progression of geographic atrophy in age-related macular degeneration imaged with spectral domain optical coherence tomography. Ophthalmology. 2011; 118:679–686. [PubMed: 21035861]
42. Zeiss CJ. Animals as models of age-related macular degeneration: an imperfect measure of the truth. Vet Pathol. 2010; 47:396–413. [PubMed: 20382825]
43. Strauss O. The retinal pigment epithelium in visual function. Physiol Rev. 2005; 85:845–881. [PubMed: 15987797]
44. Lu L, Hackett SF, Mincey A, Lai H, Campochiaro PA. Effects of different types of oxidative stress in RPE cells. J Cell Physiol. 2006; 206:119–125. [PubMed: 15965958]

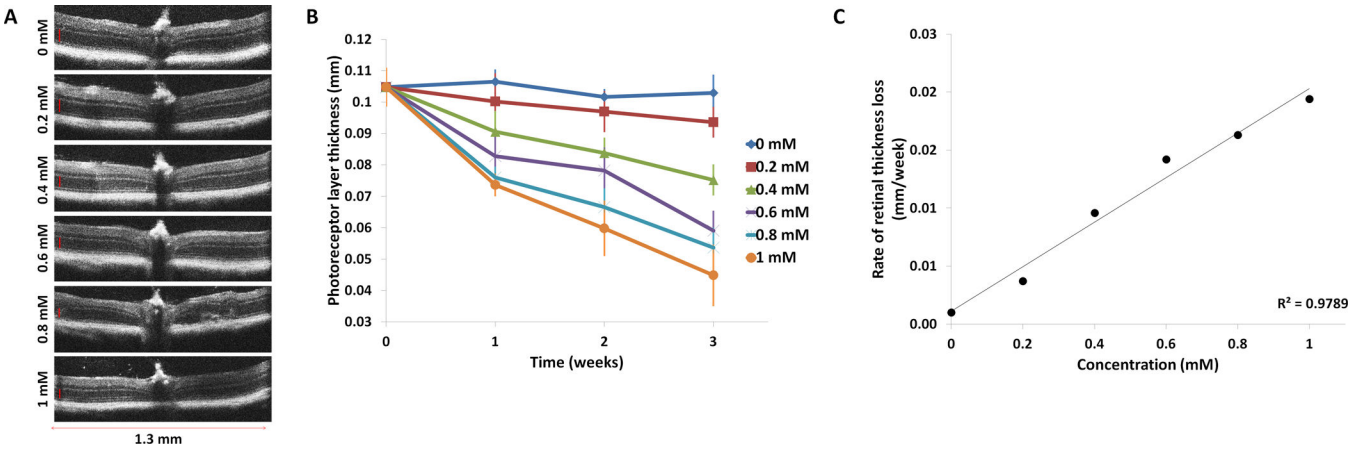

FIGURE 1. Analysis of photoreceptor layer thickness following injection of paraquat

(A) Representative OCT sections of retinas three weeks after injection of increasing concentrations of PQ. The photoreceptor layer, indicated by a vertical red line, becomes progressively thinner with increasing PQ concentration. (B) Average photoreceptor thickness across time at each concentration of PQ injected. Means ± SD are shown. PQ induced a dose-dependent reduction in photoreceptor layer thickness, measured by OCT, compared with control injections of PBS (0 mM PQ), which showed no change in photoreceptor layer thickness across the three week time course. (C) An analysis of the slopes of the linear models of degeneration at each concentration showed an increase in the rate of degeneration with respect to concentration (r^2= 0.98). Means and standard deviations are listed in Supplemental Table 1 and results of the statistical significance analysis are displayed in Supplemental Table 2.

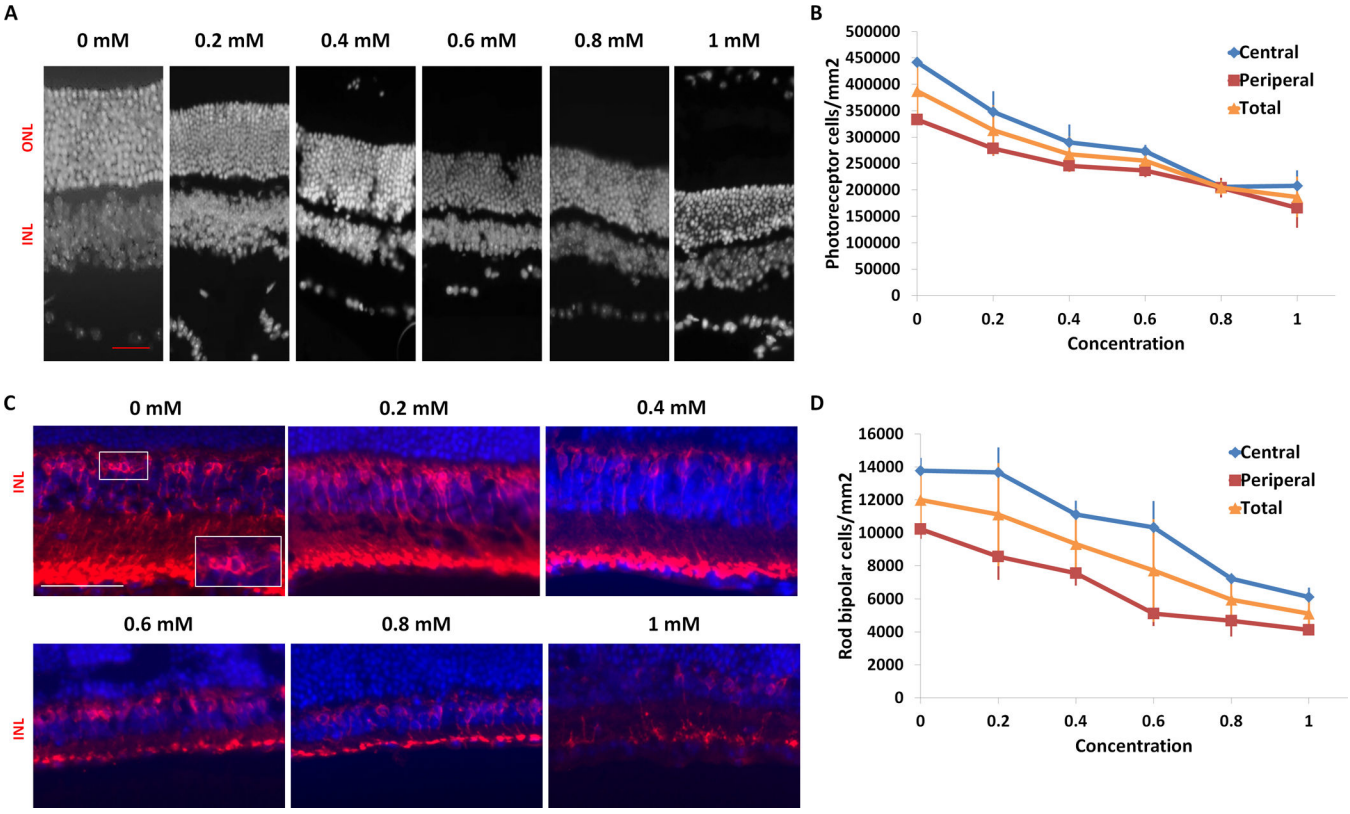

FIGURE 2. Analysis of photoreceptor loss following injection of paraquat

(A) Representative images of the nuclear layers at 3 weeks following paraquat injection. Retina sections were stained with DAPI to visualize the nuclei. There is progressive thinning of the outer nuclear layer with increasing PQ concentration. (B) Quantification of photoreceptor cells in the outer nuclear layer across the retina shows mild, but significant, photoreceptor loss in eyes injected with the lowest dose of PQ ($p<0.05$, n=3) compared with eyes injected with PBS at the 3 week time point (n=3). Photoreceptor loss progressively increased with concentration, with up to 52% degeneration at the highest concentration ($p<0.05$, n=3). A similar pattern and rate of degeneration was observed in both the central and peripheral regions of the retina. (C) Representative images of rod bipolar cells in the inner nuclear layer of the retina 3 weeks after PQ injection. Retina sections were stained for the rod bipolar cell marker PKC and counter stained with DAPI for visualization of cell nuclei. Inset in 0 mM (lower right corner) is a magnified image of the boxed region. (D) Quantification of rod bipolar cells in the inner nuclear layer of the retina shows progressive loss of bipolar cells with increasing concentration. There was up to 58% loss at the highest concentration of PQ (1 mM) compared with eyes injected with PBS (0 mM) three weeks after injections ($p<0.05$, n=3). (Scale bar = 50 μm ((A) red, (C) white); ONL, outer nuclear layer; INL, inner nuclear layer). Means ± SD are shown.

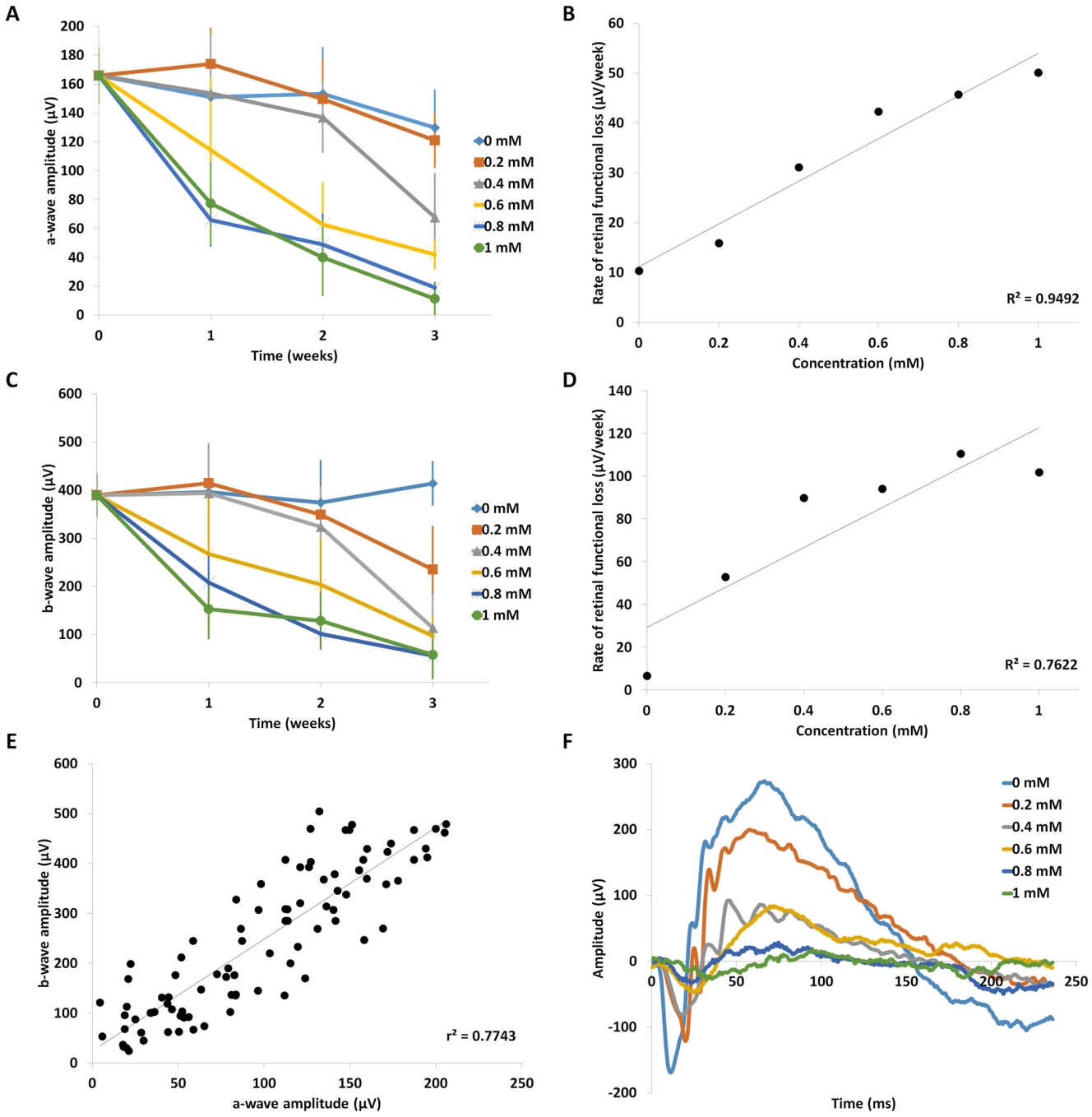

FIGURE 3. Analysis of retinal function following injection of paraquat

(A) The average amplitudes of the scotopic ERG a-wave at each PQ concentration were plotted against time. The a-wave amplitude from mice injected with PBS (0 mM PQ) showed minimal change across the three-week time course (n=5), but decreased by time and dosage in mice injected with PQ. Means ± SD are shown. Means and standard deviations are listed in Supplemental Table 1 and significance is displayed in Supplemental Table 3 (a-wave) and Supplemental Table 4 (b-wave). There was no significant change in a-wave amplitude at low concentration of 0.2 mM PQ (n=5), but reductions of a-wave amplitudes at

3 weeks post injection were significant starting at 0.4 mM ($p<0.05$, n=5), compared with 0 mM PQ. (B) The rate of ERG a-wave decline was plotted against concentration and showed a linear trend ($r^2= 0.94$). (C) The average b-wave amplitudes at each concentration were plotted against time and showed that PQ induced a time- and dose- dependent decrease. (D) The rate of degeneration of the b-wave amplitude increased in a linear manner with respect to concentration ($r^2= 0.76$). (E) Scatterplot of matched a-wave and b-wave amplitudes from individual animals at all time points and doses. Regression analysis between a-waves and b-waves showed high linear correlation ($r^2=0.77$, n=90). (F) Representative ERG waveforms (average curve from 10 flashes with an interstimulus time of 5 seconds) generated by animals three weeks after PQ injection at different concentrations are shown. The amplitudes of the peaks of the waveform become progressively smaller with increasing concentration, indicating decline in retinal function. Furthermore, the implicit times of the a-wave become greater with concentration, indicating declining retinal function with increasing PQ dose.

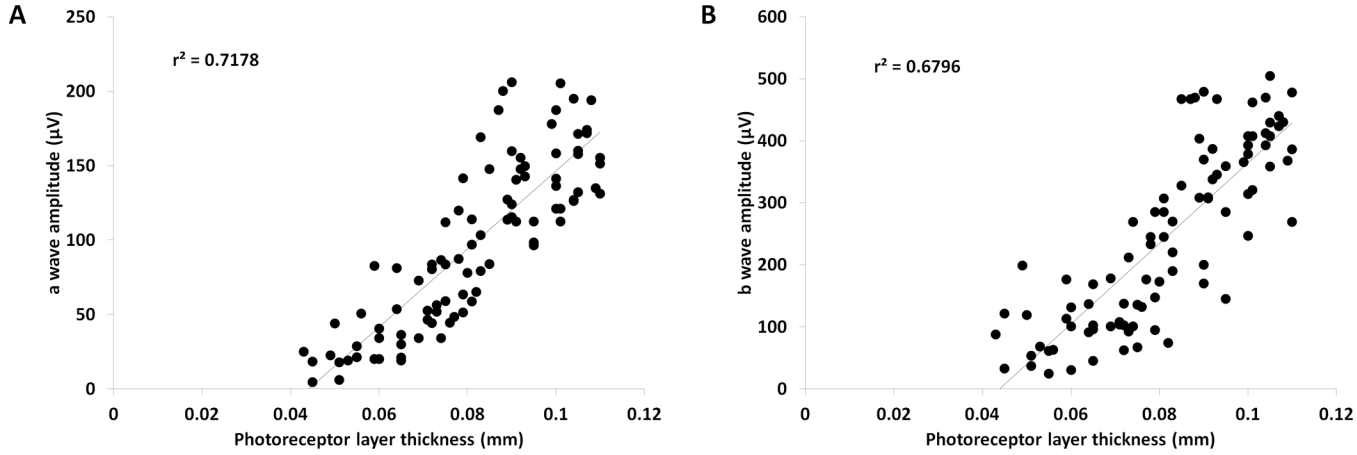

FIGURE 4. Retinal thickness correlates with retinal function

(A) A scatterplot of photoreceptor layer thickness, measured by OCT, and ERG a-wave amplitude, matched per mouse at each dose and time point, showed high positive correlation between measurements of retinal degeneration by OCT and ERG (r^2=0.72, n=90). (B) Similarly, a scatterplot of photoreceptor thickness measured by OCT and the ERG b-wave amplitude, matched per mouse at each dose and time point, also had high correlation (r^2=0.68, n=90).

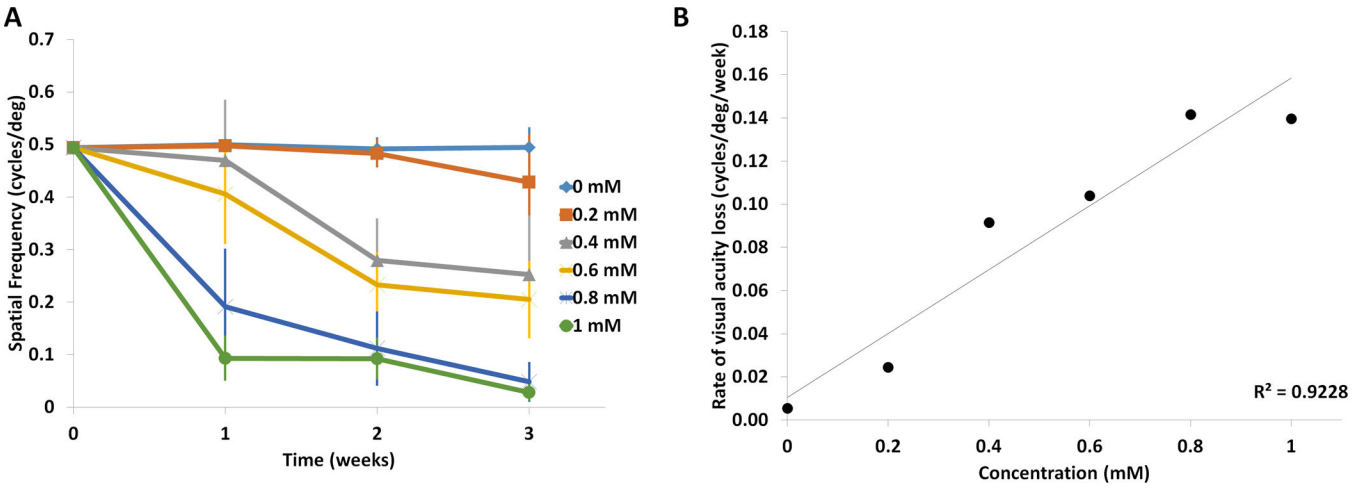

FIGURE 5. Analysis of visual behavior following injection of paraquat

(A) Paraquat induced a dose-dependent reduction in visual acuity, measured by optokinetic tracking (OKT). Visual acuity was plotted at each concentration against time. Control injection of PBS (0 mM PQ) resulted in no change in visual acuity across the three week time course (n=5). In contrast, visual acuity was reduced as the concentration of PQ increased, both time and dose dependently. Means ± SD are shown. (B) A regression analysis of the slopes of the linear models of degeneration (degeneration rate) at each concentration showed a strong linear increase in the rate of degeneration with respect to concentration (r^2= 0.92). Means and standard deviations are listed in Supplemental Table 1 and significance is displayed in Supplemental Table 5.

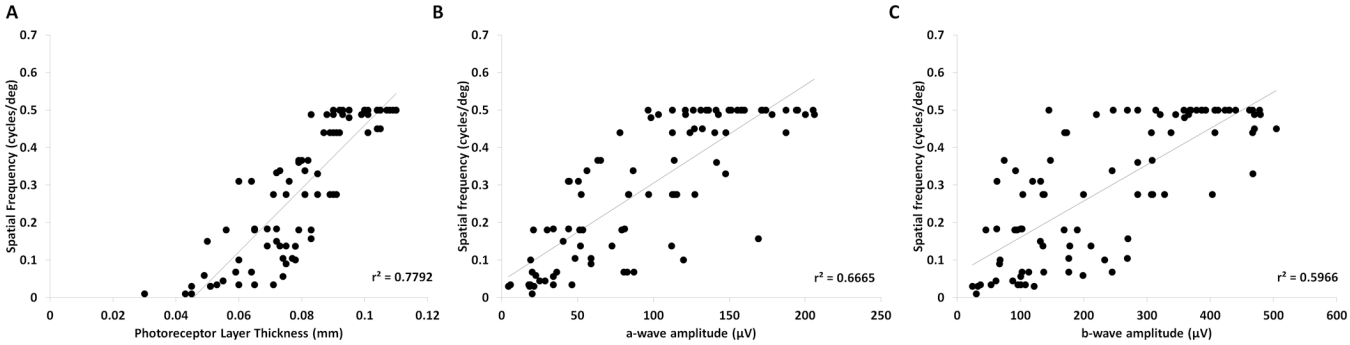

FIGURE 6. Retinal thickness and function correlate with visual acuity

(A) A scatterplot of mouse-matched photoreceptor layer thickness and visual acuity showed high positive correlation between measurements of retinal degeneration by OCT and vision by OKT (r^2=0.78, n=90). (B) A scatterplot and regression analysis of mouse-matched ERG a-wave and visual acuity showed a linear correlational trend between photoreceptor function and visual acuity (r^2=0.67, n=90). (C) A scatterplot and regression analysis of mouse-matched ERG b-wave and visual acuity. Similar to the a-wave, the ERG b-wave also had a high correlation with visual acuity (r^2=0.60, n=90).

Table 1

Rate of decline and linearity of retinal structure, function and visual behavior at different concentrations of PQ

Displayed are the slopes of the loss of structural (OCT), function (ERG a- and b-waves) and visual behavior (OKT) of the retina at various concentrations of PQ over the course of the three week time period, which indicate the rate of degeneration at each concentration (mm/week for OCT, μV/week for a-wave and b-wave, and cycles/deg/week for OKT). Lower values for the slope indicate less degeneration, while higher values indicate more degeneration. Also displayed is the coefficient of determination (r^2), which is a measure of the predictability of the decline of retinal structure, function and visual behavior.

Concentration	OCT		A-wave		B-wave		OKT	
	Slope	r2	Slope	r2	Slope	r2	Slope	r2
0 mM	−0.001	0.3927	−10.36	0.8375	6.68	0.2167	−0.0055	0.2553
0.2 mM	−0.0037	0.9928	−15.89	0.77	−52.91	0.7387	−0.0246	0.8634
0.4 mM	−0.0096	0.9743	−31.14	0.8386	−89.81	0.77	−0.0915	0.8844
0.6 mM	−0.0142	0.9505	−42.31	0.9694	−94.09	0.9873	−0.1040	0.9389
0.8 mM	−0.0163	0.9373	−45.72	0.8608	−110.53	0.9293	−0.1417	0.8596
1 mM	−0.0194	0.9577	−50.09	0.9268	−101.94	0.8353	−0.1397	0.7144

Table 2

Correlation between retinal structure, function and visual behavior at different concentrations of PQ

The slope of the line of best fit, determined by regression analysis, is shown for comparisons between the structure (OCT), function (ERG) and visual behavior (OKT) of the retina at the various concentrations of PQ over the course of the three week time period. The slope indicates the relationship between the rates of degeneration across the two measurements being compared. The coefficient of determination (r^2) indicates the variability in the difference between measurement techniques, with a higher r^2 indicating less variability.

Concentration	OCT vs a-wave		OCT vs b-wave		OCT vs OKT	
	Slope	r^2	Slope	r^2	Slope	r^2
0 mM	2232.5	0.117	3517.8	0.0441	0.0431	0.1262
0.2 mM	1382	0.2639	6470.5	0.2049	0.0408	0.2243
0.4 mM	4486.2	0.1495	14150	0.619	0.0349	0.3472
0.6 mM	2646.6	0.5376	7255.6	0.5412	0.0726	0.4128
0.8 mM	1698.4	0.6906	5296.9	0.5613	0.0829	0.512
1 mM	2086.4	0.6114	1742.3	0.1167	0.2095	0.5132
Concentration	OKT vs a-wave		OKT vs b-wave		b-wave vs a-wave	
	Slope	r^2	Slope	r^2	Slope	r^2
0 mM	275.75	0.117	−514.99	0.0625	0.4676	0.0351
0.2 mM	201.9	0.2639	616.07	0.2505	2.7425	0.7666
0.4 mM	136.96	0.1495	477.7	0.2015	2.6259	0.7641
0.6 mM	278.93	0.5376	635.92	0.3641	2.3881	0.7919
0.8 mM	221.11	0.6906	446.18	0.3064	2.103	0.4818
1 mM	745.52	0.6114	843.05	0.2443	0.9647	0.2978